Synthetic Metals 159 (2009) 1202–1209

Contents lists available at ScienceDirect

Synthetic Metals

journal homepage: www.elsevier.com/locate/synmet

Formation and degradation mechanism of a novel nanofibrous polyaniline

Ko-Shan Ho[a,*], Yu-Kai Han[a], Yu-Tsung Tuan[a], Ying-Jie Huang[b], Yen-Zen Wang[c], Tsung-Han Ho[a], Tar-Hwa Hsieh[a], Jong-Jing Lin[d], Su-Chi Lin[a,e]

[a] Department of Chemical and Materials Engineering, National Kaohsiung University of Applied Sciences, 415, Chien-Kuo Road, Kaohsiung 807, Taiwan
[b] Institute of Nanotechnology, National Chiao Tung University, 1001, Ta Hsueh Road, Hsinchu, Taiwan
[c] Department of Chemical Engineering, National Yun-Lin University of Science and Technology, 640, Yun-Lin, Taiwan
[d] General Education Division, Nan Jeon Institute of Technology, 178,Chau-Chin Road, Yen-Shui, Tainan Hsien, Taiwan
[e] Madou Junior High School, 36, Nan-Shi District, Madou, Tainan County 721, Taiwan

ARTICLE INFO

Article history:
Received 17 January 2009
Received in revised form 13 February 2009
Accepted 16 February 2009
Available online 1 May 2009

Keywords:
Polyaniline
Nanotube
Carbonization

ABSTRACT

A nanotubular, nanofibrous polyaniline (PANINT) was prepared from an emulsion polymerization in the presence of n-dodecylbenzene sulfonic (DBSA) and hydrochloric acids.

The building of the tubular structure based on the tubular micelles from the accumulation (pile up) of micelles at high surfactant concentration, leading to early stage of centipede-like and eventual tubular morphologies. The PANINT molecule owning a highly conjugated backbone demonstrated a free carrier-tail in the near-IR region due to its helical conformation. After dedoping, the once empty PANINT with only some complexed DBSA inside shrank into solid rods, after the removal of the complexed DBSA. As a result, the solid rods were filled with helical emeradine base (nano-EB) molecules associated with inter-molecular H-bonding. The solid rods of nano-EB went on crosslinking and carbonization after 200–300 °C by opening the quinoid rings and the inter-molecular H-bondings were destroyed with nano-EB molecules crosslinking into ladder-like structure. When temperature was over 300 °C and below 800 °C, carbonization enhanced by de-ammoniaization, causing a significant weight loss. However, the cleavage of aromatic rings into aliphatic pieces occurred after 800 °C, which chopped the ladder-like, strips of carbonized nano-EB sheets into small pieces of nano-particles. The conductivity of the pyrolyzed nano-EB was found to be around 10^{-5} s/cm, 10,000 times higher than the neat nano-EB of 10^{-9} s/cm due to the carbonization.

1. Introduction

Polyaniline (PANI) is a typical conducting polymer that has been found lots of applications in the field of biosensors biosensors [1], electrochemical displays [2], corrosion protection [3], rechargeable batteries [4], etc. Conventionally, to synthesize PANI via chemical oxidization [5–8] or electrochemical route [7] came out with morphology of assembled particles in which conducting PANI molecules are entangling, coiling with each other, leading to the reduction of conductivity from the interruption of conjugation. In order to obtain a PANI with higher reactive surface area, higher ordered structure, and higher conductivity, a nanofibrous or nanotube-like structure which is less possible for the molecules in it to coil or entangle with each other is necessary. Traditional chemical oxidative polymerization approaches for a nano-structured polymers include the using of insoluble solid templates such as zeolites [9], opals [10], controlled pore-size membranes [11], and anodic aluminum oxide (AAO) [12] or soluble templates such as polymers [13] and surfactants [14]. Some physical methods, such as electrospinning [15] and mechanical stretching [16] can also produce conducting polymer nanofibers without templates. When organic dopants with surfactant functionalities are used, emulsions or micelles can be formed leading to microtubes, microfibers, or microrodlike structures [17–21]. Kaner and coworkers prepared PANINT by interfacial polymerization with aniline monomers soluble in an organic solvent [22–24]. Haba et al. reported a nano-fibrous morphology of DBSA doped polyaniline originated from the filling of the nanopores of the polyaniline spherical particles into nanorods without the presence of any organic solvent, whereas the conductivity is lower due to the absence of the strong acid to induce high degree of doping [25]. Additionally, other novel meth-

* Corresponding author.
E-mail address: hks@cc.kuas.edu.tw (K.-S. Ho).

0379-6779/$ – see front matter © 2009 Elsevier B.V. All rights reserved.
doi:10.1016/j.synthmet.2009.02.047

ods like sonochemical [26] and gamma irradiation [27] methods were also used for preparation of the nano-structure of polyanilines. Stejskal et al. proposed the presence of the phenazines as the nucleus of the nanotubing in the early stage of polymerization when the pH value is still high. The phenazines behaved as the nuclei for the formation of helical polyanilines that then combined into nanofibers and dissociated from phenazines to become a separated tubes in the later stage when the pH value decreased [28].

Recently, an easy way of preparing PANINTs via emulsion polymerization in the absence of any organic solvent was developed by Ho et al. [29]. The prepared PANINT was found to be empty inside and found to be a nano-fibrous structure composed of spirally coiling polyaniline molecules [29].

It is understood that polyaniline (emeraldine base type) can undergo thermal crosslinking and becomes a ladder polymer. When the parallel helical polyaniline molecules were in the nanotube, the inter-molecular crosslinking can occur in an easier and spontaneous way between the neighboring molecules, resulting in strip like carbon sheet with built up aromatic structure when the temperature goes higher. In other words, the surface of the nanotubular polyaniline can be carbonized under thermal treatment to become materials which is competitive to carbon nanotubes.

The thermal degrading mechanism for PANINT, considered to be different from the conventional polyaniline due to its entirely different conformation [30–32], has not been studied yet. The PANINT molecules of helical conformation will demonstrate different types of thermal degradation from the conventional, non-fibrous, non-helical polyaniline as will be characterized by spectral and electronic microscopy measurements.

In this study, the thermal degradation (pyrolysis) on the PANINTs starting from room temperature to 1000 °C will be carried out in an inert atmosphere and the mechanism, carbonization will be characterized by IR, Raman spectra and morphologies of PANINTs with various thermal histories will be examined by SEM, TEM micrographs, and electron diffraction pattern, respectively.

2. Experimental

2.1. Preparation of PANINTs

To dissolve 3 g (0.091 mole) n-dodecylbenzenesulfonic acid (DBSA: TOKYO KASEI KOGYO CO.) in 50 ml de-ionized water, the mixture was slowly stirred until a homogeneous solution was formed, then 9 g (0.0968 mole) aniline monomer (TOKYO KASEI KOGYO CO.) was added and kept stirring to become emulsified then 9 ml,1 M HCl (Riedel-de Haën) was mixed with mixture, linking the micelles together and enhancing the emulsification. The mixture became turbid with the addition of HCl. An ammonium persulfate (APS: SHOWA CHEMICALS INSTRUMENT CO.) aqueous solution prepared in another beaker by dissolving 7.33 g (0.0323 mole) APS in 30 ml de-ionized water was kept in low temperature in a freezer several hours before using and was poured directly into the reaction mixture followed by a vigorous stirring with a magnetic stirrer. With the proceeding of the polymerization, the temperature rose up quickly after 10–15 min, followed by the darkening of the reaction mixture and the polymerization was proceeding for 3 h before polyaniline was isolated by filtration, followed by washing with some isopropanol and the obtained filter cakes were dried in an oven at 60 °C for 12 h.

The nano-EB was prepared by stirring PANINTs in 1 M ammonium water for more than 48 h in a magnetic stirrier. The dedoping time was found to be much longer for PANINTs compared to the regular polyaniline, which only takes at most 24 h for complete dedoping.

2.2. Prepare thermal degraded sample in a high temperature oven

An oven which can be heated up to 1000 °C was used to prepare the thermal degraded samples at various temperatures with purging argon gas.

2.3. Characterization and measurements

2.3.1. SEM (scanning electronic microscopy)

Images of PANINTs were taken in a Field Emission SEM, HR-SEM (HITACHI S-4200: accelerating voltage of 15 kV) prepared from strewn on carbonic tape and followed by posting on ferric stage.

2.3.2. TEM (transmission electronic microscopy)

Samples for field emission transmission electron microscope, HR-AEM (HITACHI FE-2000) were first dispersed in acetone and put on carbonic-coated copper grids in drop wise before subjected to the emission.

2.3.3. UV–vis-NIR spectroscopy

The UV–vis-NIR spectra of the sample were obtained from a Hitachi U-2001 and DTS-1700 NIR Spectrometer. The wavelength ranged from 300 to 1600 nm.

2.3.4. IR spectroscopy

The functional groups of neat and degraded samples were characterized by FTIR spectroscopy. The FTIR spectra were recorded on an IFS3000 v/s Fourier-transform infrared spectrometer at room temperature.

2.3.5. Raman spectroscopy

The Raman spectra of neat and degraded samples were carried out by a Triax 550 spectroscopy with a green laser light source of 520 nm wavelength. The samples were pressed into tablets before exposing to Raman source.

2.3.6. Thermogravimetric analysis (TGA)

The thermal degradation behavior of PANINT and nano-EB were characterized by a thermal gravimetric analysis of TA SDT-2960 at 10 °C/min, under purging N_2.

2.3.7. Conductivity

A 4-probes Milliohm meter (LUTRO MO-2001) was used to measure the conductivity of PANINT powders which were pressed into tablets.

3. Result and discussions

3.1. Formation mechanism of PANINTs

The SEM micrograph taken at the early stage of the polymerization demonstrated nanorods of strings made of nano-beads in Fig. 1(a), which is similar to the accumulated micelles before polymerization, as depicted in Scheme 1. These connected micelles were then polymerized into strings of beads (centipede-like) in the early stage and developed into nanofibers eventually as seen in Fig. 1(b) and depicted in Scheme 1. The obtained PANINTs were found to still retain the nano-fibrous structure after dedoping into EB-type of polyaniline in ammonia water where all the free or doped protonic acids inside or outside the tubes were removed. The dedoping caused the shrinking of the nanotube with a smaller diameter for the resultant nano-EB and the once empty PANINT became a solid rod after removing all the complexed DBSA as shown in Fig. 1(c) and Scheme 1.

The TEM image of the early stage PANINT demonstrates also the centipede-like morphology which developed into nanorods with

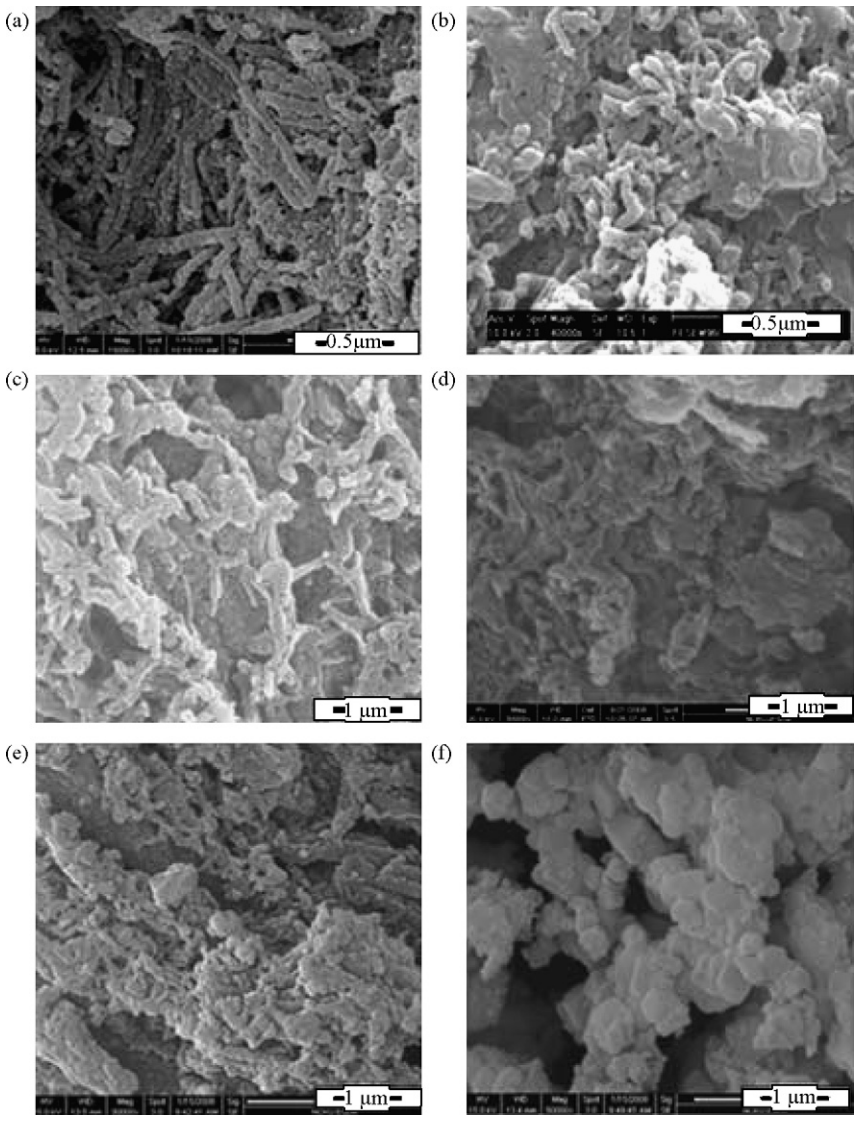

Fig. 1. SEM micrographs of (a) early stage of PANINT, (b) neat PANINT, (c) neat nano-EB, (d) neat nano-EB heated at 300 °C, (e) 600 °C, and (f) 800 °C.

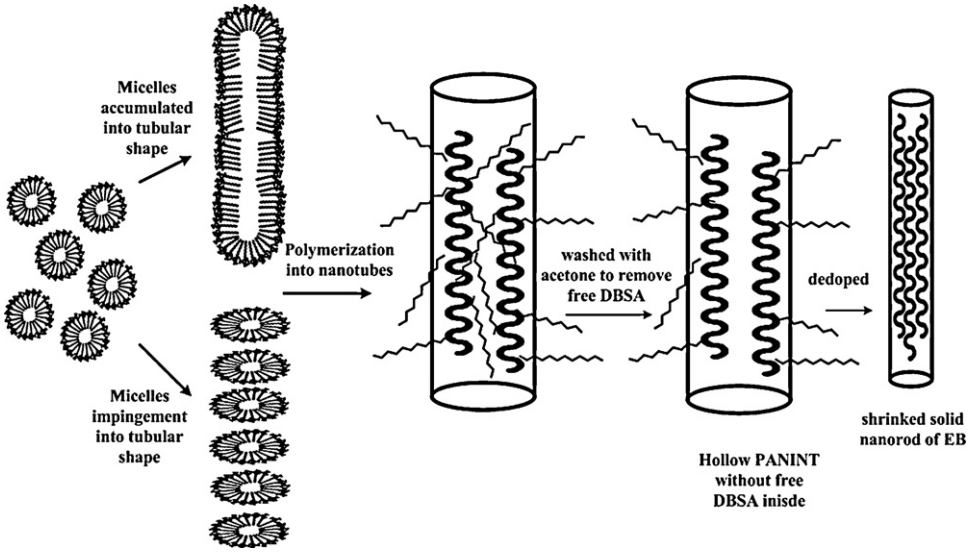

Scheme 1. Emulsion polymerization of PANINT and dedoped into nano-EB.

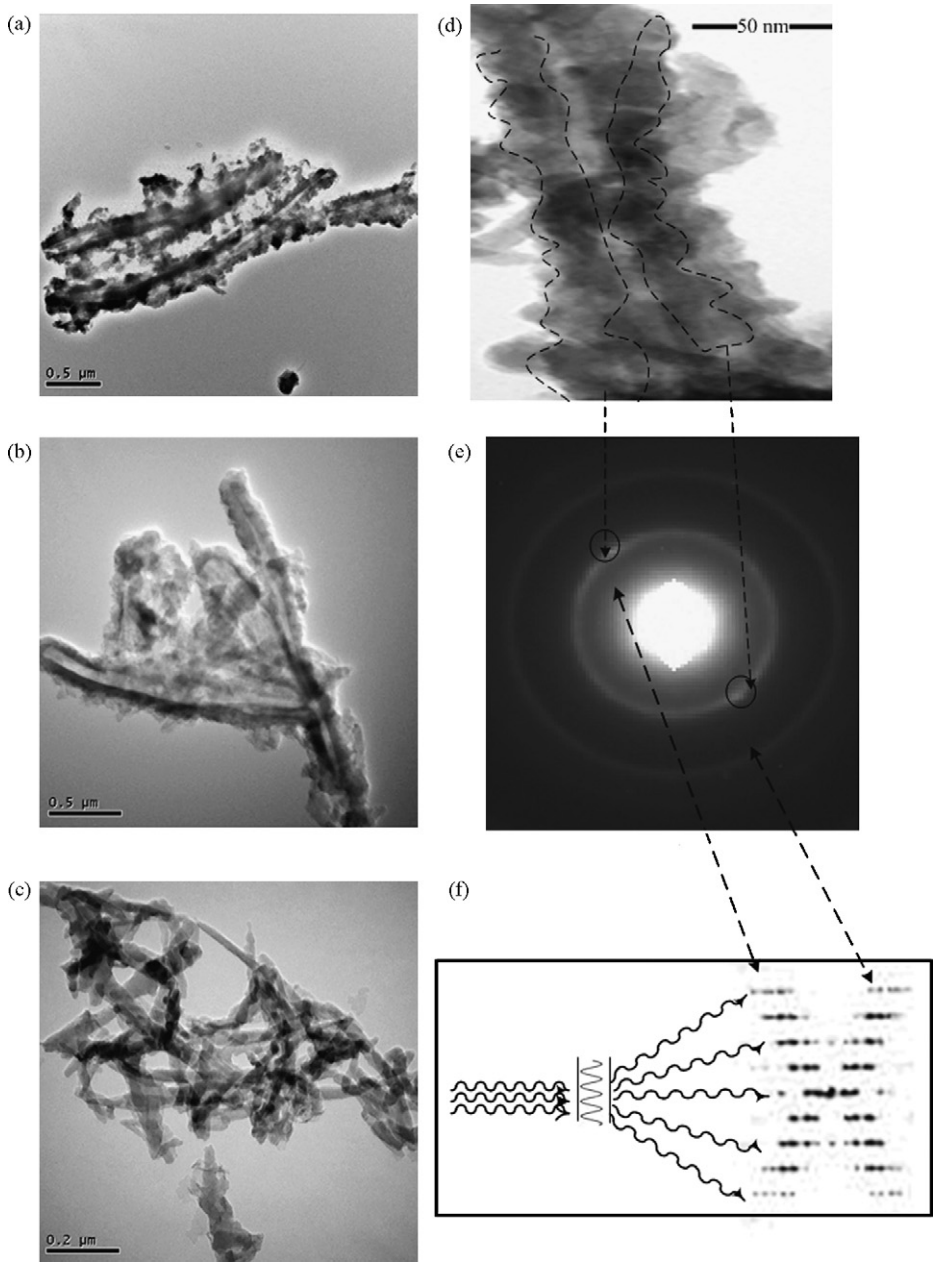

Fig. 2. TEM micrographs of (a) early stage of PANINT, (b) neat PANINT, (c) nano-EB, (d) isolated nanotube of PANINT, (e) electronic diffraction patterns of nano-EB, and (f) theoretical diffraction pattern of helical crystalline.

smoother surfaces as seen from Fig. 2(a) and (b). An isolated PANINT (ES type) is shown in Fig. 2(d) that illustrates lots of meandering, helical molecules inside the nanotube. The helical structure also demonstrated anisotropic diffraction pattern in Fig. 2(e), similar to the theoretical diffraction of helical crystalline in Fig. 2(f) and deviated from the circular pattern of common polyaniline crystals. Besides, the electron diffraction pattern is much like the helical strips prepared from the carbonization (pyrolysis) of polyacetylene [33] and template-polymerized PANINTs [34] pyrolyzed at high temperature.

The nano-EB became a smaller solid tube after dedoping as seen from its TEM micrograph in Fig. 2(c). Obviously, the diameter of the solid nanofibrous EB is significantly contracted when comparing with Fig. 2(b). After removing the complexed DBSA molecules between doped polyaniline (PANINT) molecules, the formed nano-EB molecules are able to develop strong inter-molecular H-bonding between the neighboring helixes inside the nanorods as described in Schemes 2 and 3. The helical conformation of nano-EB can be maintained and enhanced with the presence of inter-chain H-bondings depicted in Scheme 3.

3.2. Highly conjugated helical polyanilines molecules of PANINTs

The most interesting feature of the nano-polyaniline comes from the presence of the free carrier tail at the near-IR region, which is usually found when polyaniline was secondarily doped by phenolic derivatives [35–39] due to the presence of the highly conjugated, extended chain, resulting from the extension of the coiled state. Commonly, polyanilines with no secondary doping are composed of the coiled or worm-like molecules, mainly caused from the intra-complexation through the ionic bridging of the counter ions, which can effectively interrupt the conjugation and demonstrate a blue shift to the visible region. Here, in Fig. 3(a), the free carrier tail at the near-IR region can be also found for PANINT molecules in

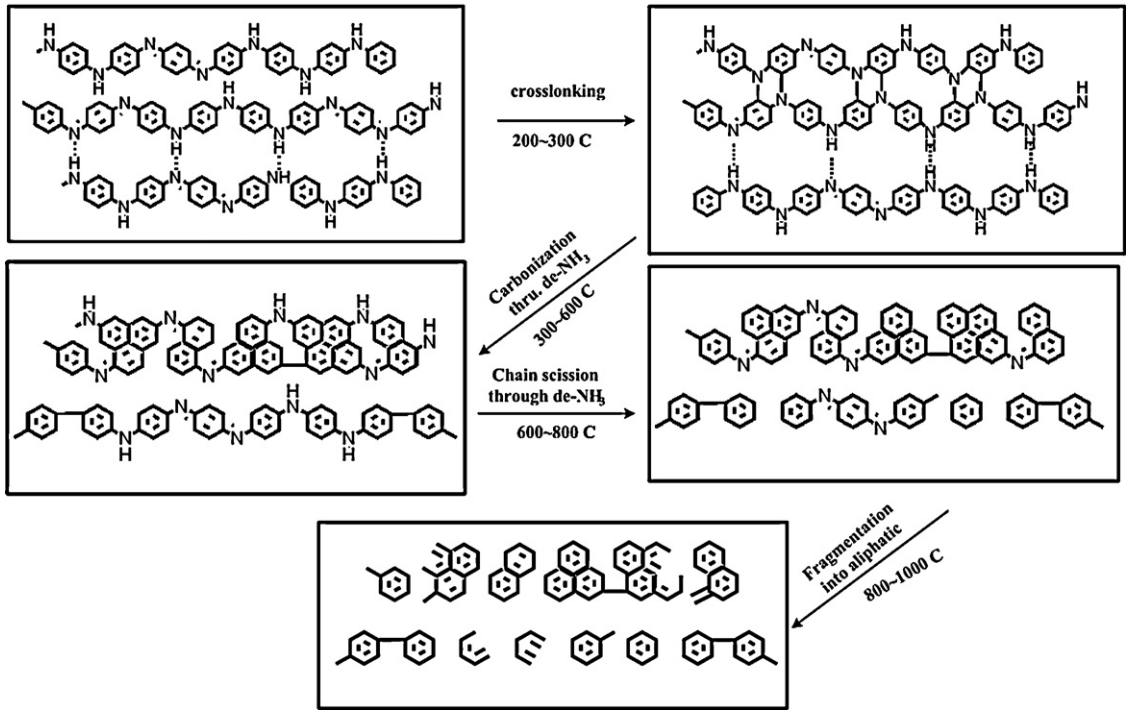

Scheme 2. Degradation mechanism of nano-EB.

the absence of any secondary doping but the formation of the helical conformation which can prevent any entanglements or coiling of the polyaniline molecules depicted in the upper in-set in Fig. 3(a). The non-interrupted conjugation was maintained through the formation of helical conformation. In other words, the PANINT molecules are helically arranged into the nanotubes and remained highly conjugated by avoiding entanglements, leading to the presence of a free carrier-tail red-shift to the higher wavelength of near-IR region shown in Fig. 3(a). And the free carrier-tail was not found in the UV–vis-NIR spectrum of random-coiled or worm-like PANIDBSA [35–39] shown in Fig. 3(b) in which only λ_{max} around 780 nm can be seen when conjugation was disrupted by the kink or entanglement of coiled chains as described in the lower in-set of Fig. 3(b). The nanotubular or nanofibrous molecules like the hairy rod molecules have a tendency to arrange into an ordered structure and give a well-defined crystalline structure as seen in the diffraction pattern found in Fig. 2(e).

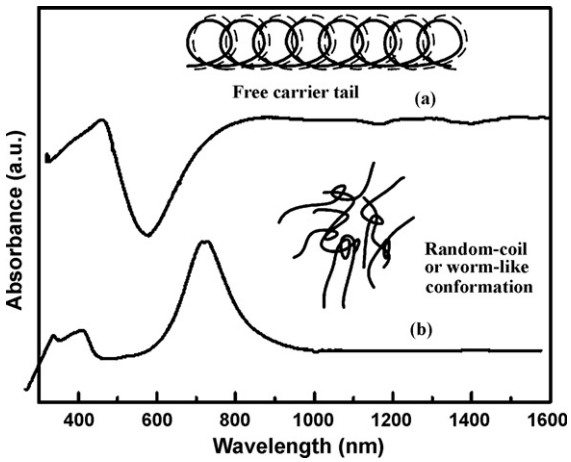

Fig. 3. UV–vis-NIR spectra of (a) PANINT and (b) DBSA doped, non-tubular polyaniline.

3.3. Characterization on the degradation mechanism of PANINTs

The DBSA emulsified micelles can associate into bigger micelles after the addition of HCl and the solution became more turbid due to the formation of bigger, micelles through the sharing of the common counter ions of the neighboring spherical micelles [29]. Lots of free or complexed DBSAs which behaved as emulsifiers will be captured inside when a tubular micelle was formed. Consequently, DBSAs free or complexed will be captured inside the polyaniline tubes after the polymerization. The free DBSAs can be removed washing with organic solvents like toluene, which can enhance the emptiness of PANINTs. And the complexed DBSAs can only be removed through the neutralization with base materials like ammonium water, which would close the empty zone of the tubes and converted the empty tubes to solid rods as described in last stage of Scheme 1.

The EB molecules inside the nanotube can be crosslinked by opening their quinone rings upon heating and the quinoid band at around 1587 cm^{-1} became shorter compared to benzenoid band at 1510 cm^{-1} when temperature is increased as seen in Fig. 4(a) and (b). The disappearance of 1380 cm^{-1} stretching mode of C–N bond of QBQ [40] in Fig. 4(b) illustrated the crosslinking of nano-EB as described in Scheme 3. And the carbonization which started at 300 °C continued when temperatures were increased to 600 and 800 °C in N_2 according to Fig. 4(c) and (d). When temperature was over 800 °C, the pyrolyzed nano-EB went on chain scission into aliphatic pieces, resulting in the significant shortening of the 1580 cm^{-1} band seen in Fig. 4(e).

Raman spectra of carbonized nano-EB at 300 °C in Fig. 5(a) shows the vibrational bands of sp^2 bonds of G-band at 1580 cm^{-1} [40], indicating some carbonization reactions already occurred at 300 °C. With the temperature increasing from 300 to 600 and 800 °C, the absorbance of bands at 1580 cm^{-1} remain higher compared to bands at 1350 cm^{-1} of G-band of disordered sp^3 carbons, indicating that the aromatic structure originated from carbonization was remained to 800 °C. However, the aromatic structure was destroyed abruptly when temperature was increased to 800–1000 °C and lots

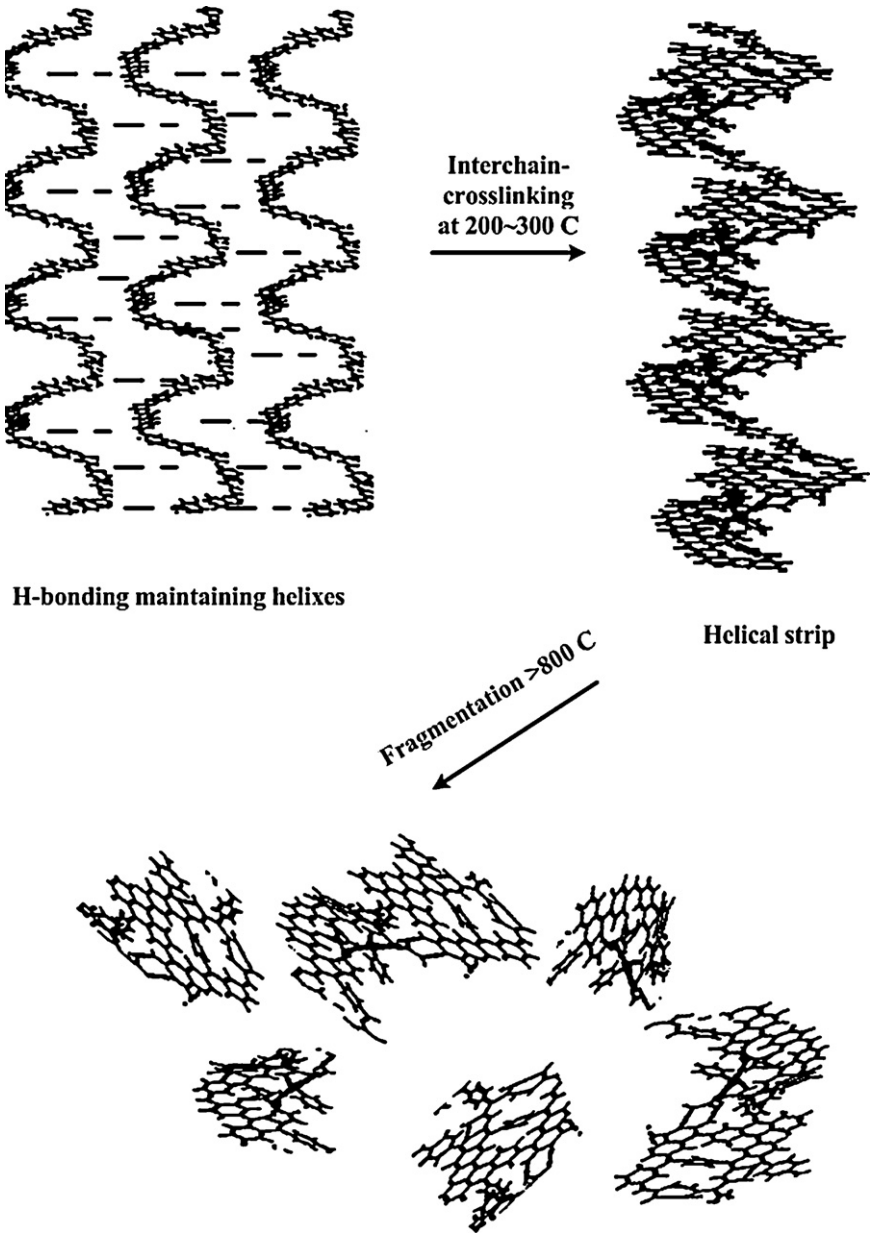

Scheme 3. Helical conformation and degradation diagram of nano-EB.

of aliphatic groups were found according to the IR-spectrum in Fig. 4(d) and (e) with the disappearance of G-band at 1580 cm^{-1} in Fig. 5(d) of Raman spectroscopy. The carbonized, crosslinked nano-EBs were cut into individual pieces by the abstract of the tertiary amine into ammonia gas that crosslinked the EB molecules together when temperature was increased to 600–800 °C. The thermal degradation behavior of nano-EB can be characterized by its thermogram obtained from TGA demonstrated in Fig. 6. It illustrates a slight weight loss around 200–400 °C from the inter-chain crosslinking, followed by a significant weight loss from 400 to 600 °C due to release of ammonia gas which can remove the nitrogen and hydrogen atoms away and leads to the carbonization process described in Scheme 2. Either the degradation (release of ammonia gas) or carbonization can cause the disappearance of the bands around 1300 cm^{-1} of C–N stretching, referring to Fig. 4(c) and (d). The carbonized residues can prevent significant weight loss from 600 to 700 °C. However, the weight loss starts again and increases steadily when temperature is over 700 °C due to the breakage of aromatic bonding as seen in Fig. 6 and Scheme 2.

3.4. Conductivity variation upon pyrolysis

The nano-EB was electrically insulated with conductivity lower than 10^{-9} S/cm, which cannot be measured by a regular mini-ohm meter. However, its conductivity can be increased to 10^{-5} S/cm and can be measurable from the mini-ohm meter after staying in the high temperature oven for 30 min at 800 °C with purging argon gas. The conductivity was not found to be still too compared with carbon nanotubes when the conjugated aromatic rings broke into aliphatic pieces made of non-conjugated C–C structures at 800–1000 °C seen in Fig. 4(e) and described in Schemes 2 and 3. High temperature (pyrolysis) does improve the conductivity by carbonization but chain scission degradation was also present to break the conjugation and decrease the conductivity since the chain scissions at high temperature mostly results in the formation of C–C single bonds

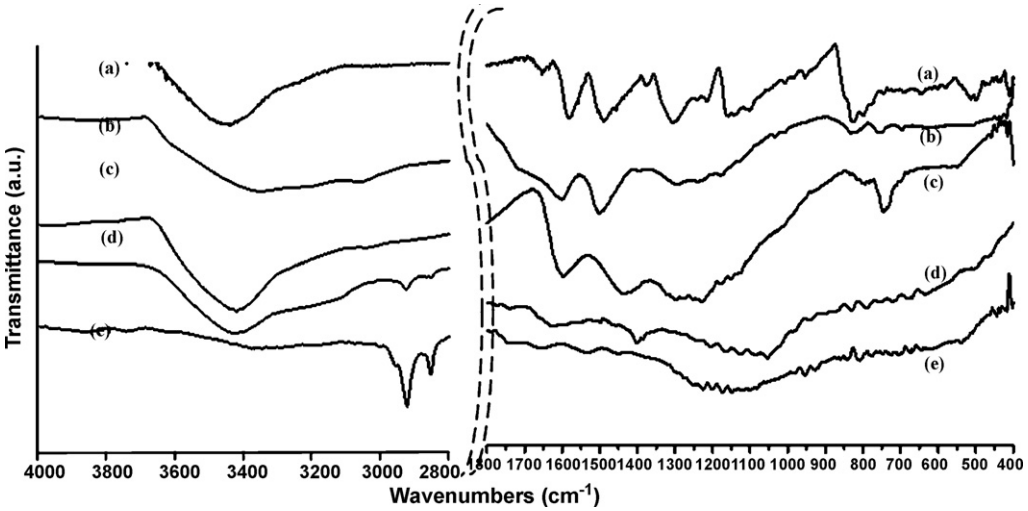

Fig. 4. IR spectra of nano-EB at (a) RT, (b) 300 °C, (c) 600 °C, (d) 800 °C, and (e) 1000 °C.

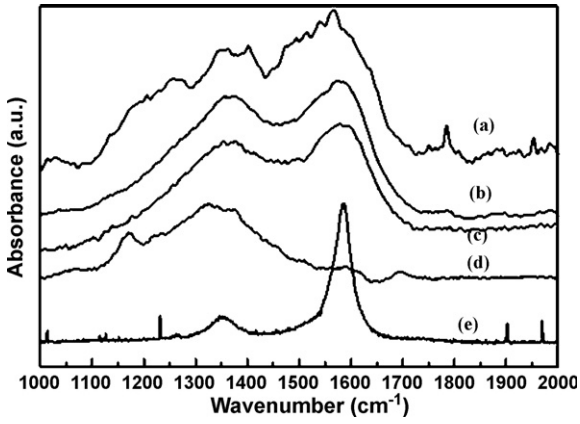

Fig. 5. Raman spectra of nano-EB at (a) 300 °C, (b) 600 °C, (c) 800 °C, and (d) 1000 °C.

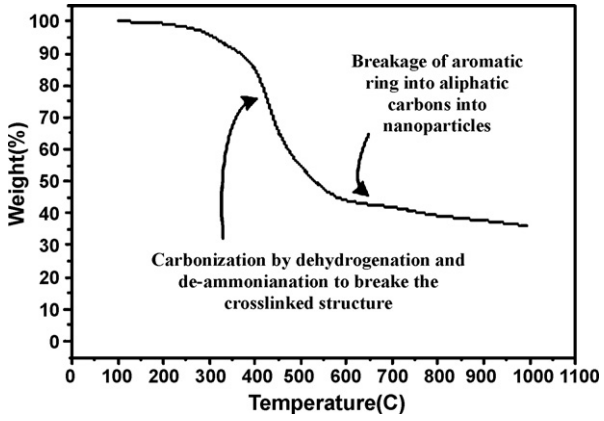

Fig. 6. TGA thermogram of nano-EB.

(sp^3) not C=C double bonds (sp^2) that can enhance the conjugation and conductivity.

4. Conclusion

A nanotubular polyaniline can be prepared directly from the emulsion polymerization of anilinium salt in the presence of DBSA and HCl. The electronic micrographs at each stage of polymerization illustrated the formation of nanotubes from the accumulation or impingement of micelles before or during polymerization. The prepared PANINTs were found to own a highly conjugated backbone, leading to the strong red shift and the appearance of a carrier-tail like spectrum at NIR region due to its non-entangled, non-coiled helical conformation.

Nanotubular PANINTs were dedoped into solid, nanorods of EB type polyaniline molecules which still own helical conformation. These nano-EB molecules went on crosslinking type of degradation when temperature was increased, followed by carbonization through the release of ammonia gas at higher temperature. The carbonization confirmed by both IR and Raman spectra resulted in the increase of the conductivity of nano-EB after pyrolysis. However, some chain scissions occurred after 800 °C, interrupted the conductivity increase of the pyrolyzed EB.

In the future, various naorods of EB will be prepared and thermal degradation at temperature higher than 1000 °C will be carried out to obtain a highly conductive, processible pyrolyzed EB to replace the intractable, insoluble carbon nanotubes.

References

[1] A. Ambrosi, A. Morrin, M.R. Smyth, A.J. Killard, Anal. Chim. Acta 609 (2008) 37.
[2] K. Brazdziuviene, I. Jureviciute, A. Malinauskas, Electrochim. Acta 53 (2007) 785.
[3] Y.Y. Wang, X.L. Jing, Polym. J. 36 (2004) 374.
[4] K. Ghanbari, M.F. Mousavi, M. Shamsipur, H. Karami, J. Power Sources 170 (2007) 513.
[5] A.J. Epstein, J.M. Ginder, F. Zuo, R.W. Bigelow, H.S. Woo, D.B. Tanner, A.F. Richter, W.S. Huang, A.G. Macdiarmid, Synth. Met. 18 (1987) 303.
[6] A.G. MacDiarmid, A.J. Epstein, Faraday Discuss., Chem. Soc. 88 (1989) 317.
[7] A.G. MacDiarmid, J.-C. Chianig, A.F. Richter, N.L.D. Somasiri, A.J. Epstein, Conductive Polymers, first ed., Dordrecht, 1987, p. 105.
[8] W.S. Huang, B.D. Humphrey, A.G. MacDiarmid, J. Chem. Soc., Faraday Trans. I 82 (1986) 2385.
[9] C.G. Wu, T. Bein, Stud. Surf. Sci. Catal. 84 (1994) 2269.
[10] V. Misoska, W. Price, S. Ralph, G. Wallace, Synth. Met. 121 (2001) 1501.
[11] V.M. Cepak, C.R. Martin, Chem. Mater. 11 (1999) 1363.
[12] J. Jang, J. Bae, Adv. Funct. Mater. 15 (2005) 1877.
[13] M.R. Simmons, P.A. Chaloner, S.P. Armes, Langmuir 11 (1995) 4222.
[14] Y.L. Lee, J.I. Shin, K.W. Park, C.E.R. Holze, J. Appl. Polym. Sci. 88 (2003) 1550.
[15] A.G. MacDiarmid, W.E. Jones, I.D. Norris, J. Gao, A.T. Johnson, N.J. Pinto, J. Hone, B. Han, F.K. Ko, H. Okuzaki, M. Llaguno, Synth. Met. 119 (2001) 27.
[16] H. He, C.Z. Li, N.J. Tao, Appl. Phys. Lett. 78 (2001) 811.
[17] P.J. Kinlen, J. Liu, Y. Ding, C.R. Graham, E.E. Remsen, Macromolecules 31 (1998) 1735.
[18] Z.X. Wei, Z.M. Zhang, M.X. Wan, Langmuir 18 (2002) 917.
[19] Z.X. Wei, M.X. Wan, J. Appl. Polym. Sci. 87 (2003) 1297.
[20] J.J. Langer, G. Framski, R. Joachimiak, Synth. Met. 121 (2001) 1281.
[21] H.J. Qiu, M. Wan, X.B. Matthews, L.M. Dai, Macromolecules 34 (2001) 675.
[22] S. Virji, J.X. Huang, R.B. Kaner, B.H. Weiller, Nano Lett. 4 (2004) 491.
[23] J.X. Huang, R.B. Kaner, J. Am. Chem. Soc. 126 (2004) 851.
[24] J.X. Huang, S.B. Virji, H. Weiller, R.B. Kaner, J. Am. Chem. Soc. 125 (2003) 314.

[25] Y. Haba, E. Segal, M. Narkis, G.I. Titelman, A. Siegmann, Synth. Met. 106 (1999) 59.
[26] X.L. Jing, Y.Y. Wang, D. Dan Wu, L. She, Y. Guo, J. Polym. Sci. Chem. Ed. 44 (2006) 1014.
[27] S.K. Pillalamarri, F.D. Blum, A.T. Tokuhiro, J.G. Story, M.F. Bertino, Chem. Mater. 17 (2005) 227.
[28] J. Stejskal, A. Riede, D. Hlavata, J. Prokes, M. Helmstedt, P. Holler, Synth. Met. 96 (1998) 55.
[29] B.Z. Hsieh, H.Y. Chuang, L. Chao, Y.J. Li, Y.J. Huang, P.H. Tseng, T.H. Hsieh, K.S. Ho, Polymer 49 (2008) 4218.
[30] T.C. Tsai, D.A. Tree, M.S. High, Ind. Eng. Chem. Res. 33 (1994) 2600.
[31] C. Yang, Z. Fang, J. Liu, W. Liu, H. Zhou, Thermochim. Acta 352–353 (2000) 159.
[32] K. Luo, N.L. Shi, S. Chao, Polym. Degradation Stability 91 (2006) 2660.
[33] M. Kyotani, S. Matsushita, T. Nagai, Y. Matsui, M. Shimomura, A. Kaito, K. Akagi, J. Am. Chem. Soc. 130 (2008) 10880.
[34] M. Kyotani, H. Goto, K. Suda, T. Nagai, Y. Matsui, K. Akagi, J. Nanosci. Technol. 8 (2008) 1999.
[35] K.S. Ho, T.H. Hsieh, C.W. Kuo, S.W. Lee, Y.J. Huang, C.N. Chuang, J. Appl. Polym. Sci. 103 (2006) 2120.
[36] K.S. Ho, Synth. Met. 126 (2002) 151.
[37] L. Chao, Y.K. Han, B.Z. Hsieh, Y.J. Huang, T.H. Hsieh, C.M. Lin, S.Z. Lin, P.H. Tseng, K.S. Ho, J. Appl. Polym. Sci. 108 (2008) 3516.
[38] C.S. Wu, Y.J. Huang, T.H. Hsieh, P.T. Huang, B.Z. Hsieh, Y.K. Han, K.S. Ho, J. Polym. Sci. Chem. Ed. 46 (2008) 1800.
[39] L. Chao, Y.J. Huang, Y.K. Han, P.H. Tseng, T.H. Hsieh, C.M. Lin, K.S. Ho, Polym. Bull. 60 (2008) 847.
[40] V. Baranauskas, H.J. Ceragioli, A.C. Peterlevitz, J.C.R. Quispe, J. Phys. Conf. Series 61 (2007) 71.